JOURNAL OF MATERIALS SCIENCE 20 (1985) 1275–1284

Debonding and pull-out processes in fibrous composites

J. K. WELLS*, P. W. R. BEAUMONT
Cambridge University Engineering Department, Trumpington Street, Cambridge, UK

The processes of debonding and pull-out in fibrous composites are described. Models predicting the debond length and the probability distribution of pull-out lengths of fibres and bundles are derived. These lengths are functions of the fibre, matrix and interface properties. Prediction is then compared with experiment and a simple relationship between pull-out and debond lengths is found. An understanding of the debonding and pull-out processes is important because they affect the fracture toughness of fibre composites.

1. Introduction

The impact toughness of a fibre-reinforced polymer composite is higher than that of either of its constituent phases. A number of reasons have been proposed [1–3] based on the processes of fibre pull-out and debonding which absorb energy in the composite. This paper analyses the fracture of a composite, enabling the pull-out and debonding lengths to be calculated. These processes can operate not only on single fibres, but also on bundles of fibres.

2. Description of the failure processes

Consider a composite of continuous fibres aligned parallel to an applied load (Fig. 1). Perpendicular to the fibre direction is a notch. Under monotonic loading the material at the notch-tip fractures and a small crack forms in the matrix. Load, once carried by the matrix, is transferred by shear to the fibres which are still intact. These shear forces eventually become so large that the bond between fibre and matrix fails. A cylindrical crack at the interface propagates from the matrix crack surface along the fibre as the applied load increases. This process is called *debonding*.

Some load transfer between fibre and matrix is still possible by interfacial forces due to matrix shrinkage on to the fibre during manufacture. This friction produces a non-uniform stress along the debonded fibre. Because of the variable strength of the fibre along its length, the fibre is able to break some distance from the matrix crack-plane where the stress is highest. After fracture, the composite typically shows a matrix crack-plane with fibres protruding from it. This process is called *pull-out*.

3. The process of debonding

The process of debonding is controlled by two parameters: the fibre debond stress, and the rate of increase of stress along the length of debonded fibre due to friction. After the matrix cracks, the fibre stress at the interfacial (debond) crack front is the debond stress σ_d, and the applied fibre stress when a length x has debonded is

$$\sigma(x) = \sigma_d + f(x) \quad (1)$$

where $f(x)$ is the stress in the fibre caused by friction on its surface. When $\sigma(x)$ reaches the ultimate strength of the fibre, σ_f, failure occurs and the debond length may be determined provided σ_d and $f(x)$ are known.

3.1. Calculation of the debond stress

The debond stress can be predicted using a shear-lag analysis [4–6]. The shear stress at the interface can be calculated as a function of applied load, assuming debonding occurs when the shear strength of the interface τ_0, is exceeded. In [4–6] similar results are obtained; for example Takaku

Present address: BP Research Centre, Chertsey Road, Sunbury-on-Thames, Middlesex, UK.

0022–2461/85 $03.00 + .12 © *1985 Chapman and Hall Ltd.*

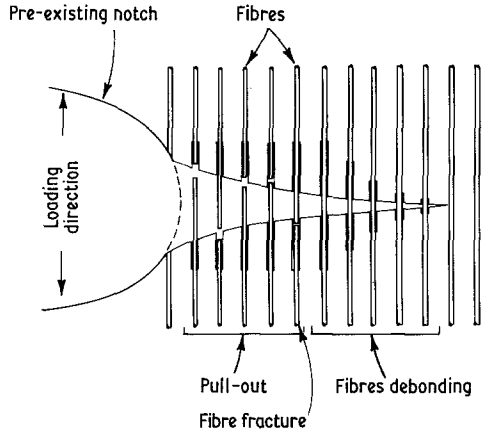

Figure 1 Schematic diagram of composite fracture ahead of a notch.

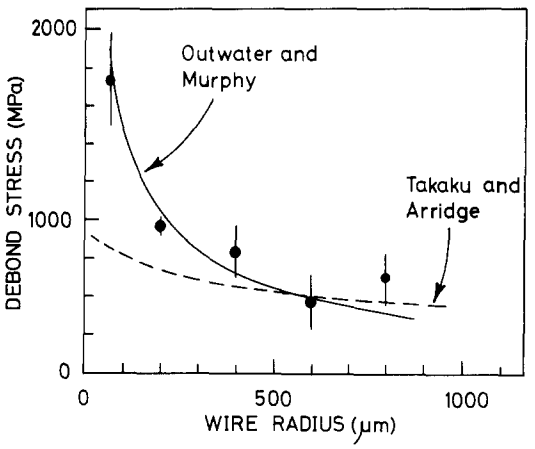

Figure 2 Variation of debond stress with wire radius. Solid line: debond stress calculated from Equation 3 with $E_f = 210\,\text{GPa}$ and $G_{2c} = 200\,\text{J m}^{-2}$. Dashed line: debond stress from Equation 2 with $G_m = 1.1\,\text{GPa}$, $\tau_0 = 20\,\text{MPa}$, $r_m = 10\,\text{mm}$.

and Arridge [6] predict that

$$\sigma_d \simeq 2\tau_0 \left(\frac{E_f}{2G_m}\right)^{1/2} \left[\ln\left(\frac{r_m}{r_f}\right)\right]^{1/2} \quad (2)$$

where E_f is the Young's modulus of the fibre and G_m the matrix shear modulus. Other derivations also agree on the dependence of debond stress on τ_0, E_f and G_m. The function involving fibre radius, r_f, and the effective radius of its surrounding matrix cylinder, r_m, depends on the precise fibre geometry considered.

Such stress-based analyses have the disadvantage of taking no account of any stress concentration at the crack front and may, therefore, overestimate the debond stress. An alternative approach based on the energetics of failure is described by Outwater and Murphy [7], where

$$\sigma_d = \left(\frac{4E_f G_{2c}}{r_f}\right)^{1/2} \quad (3)$$

G_{2c} is the mode 2 critical-strain energy release rate for interfacial cracking. Outwater and Murphy's derivation of this equation is confusing since they do not state whether the model is in the fixed-grips or fixed-load condition. Wells [8] re-derived their model to clarify this point. Clearly, only if there is both sufficient stress to nucleate an interfacial crack and a favourable energy balance can the crack propagate.

The most convenient way of distingushing between Equations 2 and 3 is to experimentally investigate the dependence of debond stress on fibre radius. Wells [8] therefore measured the debond stress of steel wires of varying diameter embedded in epoxy resin, and the results are shown in Fig. 2. We see that the debond stress is more accurately predicted by the energy condition.

3.2. Interfacial frictional stress transfer

The frictional stress transfer between fibre and matrix is due to compressive radial stress produced both by the shrinkage of the resin during cure, and by thermal mismatch effects during cooling. The radial stresses can be estimated by a simple analysis developed by Harris [9], although the model does not take into account the constraining effects of surrounding fibres.

3.2.1. Simple linear model

If a fibre is assumed infinitely stiff, there is no Poisson contraction transverse to the direction of applied load, and the frictional interfacial stress is uniform. The stress in a fibre embedded to a distance x is therefore

$$\sigma(x) = \frac{2\pi r_f \tau_f x}{\pi r_f^2} = \frac{2\tau_f x}{r_f}$$

where $\tau_f = \mu P$; μ is the coefficient of friction between fibre and matrix and P is the average radial compressive stress around the fibre. This approximation has been used extensively in the literature.

3.2.2. Non-linear model

Although fibres are generally stiff, the simple linear model overestimates the frictional stress transfer because Poisson contraction cannot be

ignored. Full allowance for this effect is made in the derivation of Wells [8], which shows that

$$\sigma(x) = \sigma_p(1 - \sigma^{-\beta x}) \quad (4)$$

where

$$\sigma_p = \frac{\epsilon_0 E_f}{\nu_f} \qquad \beta = \frac{2\mu\nu_f E_m}{E_f r_f(1+\nu_m)}$$

ν and E are the Poisson's ratio and Young's modulus of fibre and matrix (subscripts f and m respectively), μ is the coefficient of friction between fibre and matrix, r_f the fibre radius and ϵ_0 the "misfit strain" between fibre and matrix. Equation 4 predicts that the rate of stress build-up will fall as the axial fibre load increases. The maximum shear stress that can be produced by frictional loading is σ_p, when the Poisson contraction of the fibre is equal to the residual strain of the matrix.

If the origin of the coordinates is taken as the debond crack front at which the fibres stress is σ_d, then Equation 4 becomes

$$\sigma(x) = \sigma_p - (\sigma_p - \sigma_d)e^{-\beta x} \quad (5)$$

3.3. Calculation of the debond length

Failure of a fibre of uniform strength occurs when the stress in that portion of fibre between the matrix crack surfaces reaches the strength of the fibre, σ_f. The debond crack ceases to propagate and the debonded length, l_d, is therefore given by the condition

$$\sigma_f = \sigma_p - (\sigma_p - \sigma_d)^{-\beta l_d/2}$$

and hence

$$l_d = \frac{2}{\beta}\ln\left|\frac{\sigma_p - \sigma_d}{\sigma_p - \sigma_f}\right|$$

where l_d is the final debonded length on both sides of the matrix crack (Fig. 3). If $\sigma_d > \sigma_f$ no debonding occurs; if $\sigma_f > \sigma_p$ and $\sigma_f > \sigma_d$, debonding extends along the entire length of fibre.

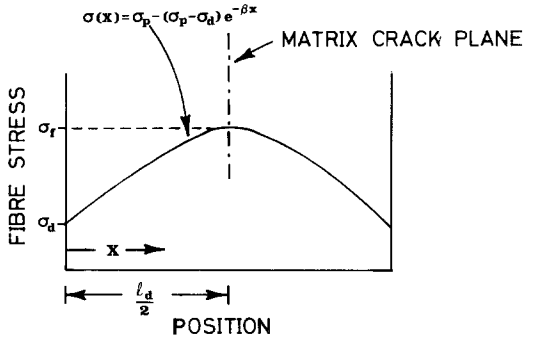

Figure 3 Calculation of the debond length.

3.4. Effect of reinforcement on the nature of debonding

Equation 3 predicts that low-stiffness or large-radius fibres will have a low debond stress. Consequently, a phenomenon which may be called "bundle debonding" can occur. This process may operate even though the fibre debond stress exceeds the fibre strength, and no individual fibre debonding would be predicted. Bundles consist of a group of fibres bonded by resin. They behave as large single fibres. Such a bundle has a lower stiffness and strength than a single fibre, but with a larger radius. The interfacial parameter G_{2c} will also be a combination of the pure matrix and interface properties.

After debonding a bundle will have a corrugated surface, and therefore any small movement of the bundle with respect to its "socket" will cause interlocking of these corrugations. This will produce an effective residual compressive strain on the bundle of fibres, similar to that of the single-fibre case. The stress distribution and debond stress of a bundle may be approximated by Equations 3 and 5 after substitution of the relevant material properties. These corrugations may also provide an airgap which accounts for the whitening observed in debonded glass-fibre composites. A debonded single fibre would not produce a sufficiently large airgap to create such whitening effects.

3.4.1. Calculation of bundle properties for calculation of bundle debond length

The bundle stiffness and strength may be calculated using the rule of mixtures, where the fracture of weak fibres reduces the strength of the bundle to 80% of the ideal rule-of-mixtures prediction [10]. Poisson's ratio of a bundle is that of a typical composite of appropriate fibre volume fraction ($\nu = 0.32$).

The interface parameter G_{2c} is assumed to be a linear function of the two constituent material properties:

$$G_{2c} = \frac{1}{a}|\pi r_f G_1 + (a - 2r_f)G_2| \quad (7)$$

where G_1 and G_2 are the critical energy release rates for fracture of interface and pure resin respectively. The spacing a between fibre centres

TABLE I Variation in debond lengths with specimen type

Specimen type	No. of specimens	Debond length (mm)		Notes
		Observed	Predicted	
A	30	2.7 ± 0.2	3.9	$V_f = 23\%$ $r_b = 0.5$ mm
B	90	5.8 ± 0.6	7.9	$V_f = 40\%$ $r_b = 0.45$ mm
C	10	7.1 ± 1.0	8.7	As B with $G_i = 0$

around the edge of the bundle is given by the square-packing approximation

$$a \simeq \left(\frac{\pi r_f^2}{V_f}\right)^{1/2} \quad (8)$$

where V_f is the volume fraction of fibres in the bundle.

Wells [8] measured $G_2 \simeq 500\,J\,m^{-2}$ for an epoxy resin matrix and G_1 approximately 50, 2 and $60\,J\,m^{-2}$ for E-glass, Kevlar, and high-strength carbon fibres in epoxy respectively. The misfit strain between bundle and matrix was found to be about 5%, and the radius of a bundle r_b was typically 500 μm.

3.5. Comparison of observed and predicted debond lengths in model composites

Experiments have been carried out on model composite specimens, where debond lengths may be accurately measured and compared with theoretical predictions. The specimens have been described previously [3]. Briefly, a specimen consisted of a single layer of glass reinforcing tows, situated close to the tensile side of a small epoxy beam loaded in three-point bending. The observed lengths of bundle debonding are shown in Table I, each result being the average of at least 100 measurements (ten measurements per specimen). Results for specimens of three types are presented:

(a) Type A had no weft fibres holding the main tows in place, enabling bundle spreading to occur during manufacture.

(b) Type B had a small number of light weft fibres present, holding the bundle together and reducing the interfibre spacing. This corresponds to a composite with a locally higher volume fraction.

(c) Type C were specimens prepared as Type B but the fibres were sprayed with mould release fluid, producing a weak fibre/matrix bond.

Table I also shows the predicted debond lengths using Equations 3, 6, 7 and 8, with substitution of material properties listed in Table II. Values of G_1, G_2, and misfit strain ϵ_0, are those reported in the previous section, except in the case of Type C specimens where it is assumed that no fibre–matrix bonding occurred and consequently $G_1 = 0$ in this case. Agreement between observed and predicted values is generally good, although the predictions are typically 30% higher than the observed values.

4. The process of pull-out

The fundamental origin of pull-out is the variable strength of the reinforcing fibre. In the absence of strength-reducing flaws a fibre would break in the region of maximum stress (i.e. between the faces of a matrix crack), and no pull-out would result. However, when a brittle fibre carries a non-uniform load along its length the fibre may either fracture at a large flaw in a region of low stress, or at a minor flaw at a point of higher stress. This is shown schematically in Fig. 4. In this case fibre fracture will occur at point A away from the region of maximum stress, and will produce pull-out during crack propagation.

4.1. A statistical model for pull-out

After the matrix cracks, the load on a fibre close to the crack tip increases causing debonding. Friction between fibre and matrix gives rise to a non-uniform stress distribution along the fibre

TABLE II Properties of fibres and epoxy resin

Material	Strength (MPa)	Young's Modulus (GPa)	Radius (μm)	Poisson's ratio
Glass fibre	1650	70	7	0.2
Carbon fibre	2480	230	4	0.2
Resin	80	3	–	0.35

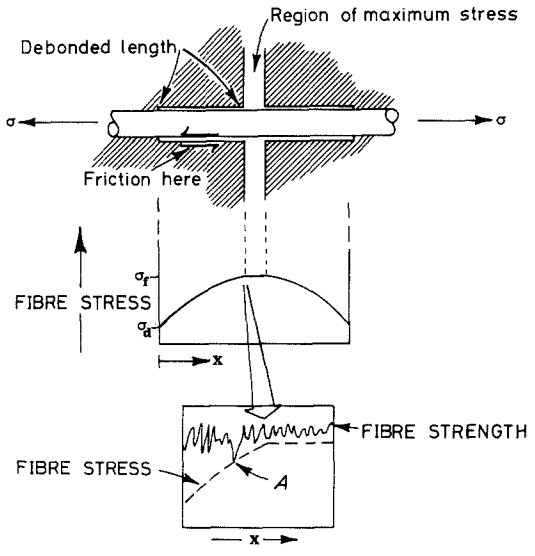

Figure 4 Schematic diagram showing origin of pull-out.

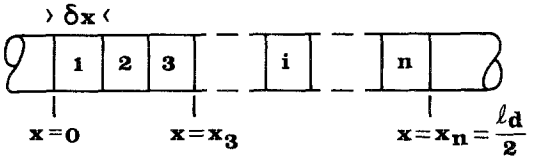

Figure 5 Schematic diagram of debonded fibre.

the sum of $[1-P(\sigma_j)]$ for all $j > i$, i.e. all sections more highly loaded than section i*.

The relative probability of fracture occurring in section i is therefore given by

$$f_i \propto P(\sigma_i) \sum_{j=i+1}^{n} [1-P(\sigma_j)]\,\delta x \qquad (10)$$

Equation 10 may be re-expressed to present an integral form of the cumulative probability function

$$F(x) = \int_0^x P[\sigma(x')]\left(\int_{x'}^{l_d/2}\{1-P[\sigma(x'')]\}\,dx''\right)dx' \Big/ \int_0^{l_d/2} P[\sigma(x')]\left(\int_{x'}^{l_d/2}\{1-P[\sigma(x'')]\}dx''\right)dx' \qquad (11)$$

length. The variable strength of a brittle fibre is controlled by the distribution of flaws along its length. Experiments show that the strength of such material is well described by a Weibull distribution. On loading the material up to a stress σ, a fraction of the fibres $P(\sigma)$ will fail; in its simplest form

$$P(\sigma) = 1-\exp\left[-(\sigma/\sigma_0)^m\right] \qquad (9)$$

where σ_0 is a characteristic strength and m the Weibull modulus.

Consider a debonded fibre with a series of sections of length δx to be non-uniformly loaded as in Fig. 5. The stress in the ith section increases from zero to σ_i as the debond crack propagates along the fibre. The nth section is at the point of maximum fibre stress, i.e. in the plane of the matrix crack. The probability of failure in loading section i from zero load to σ_i is given by the cumulative probability of failure $P(\sigma_i)$.

However, the probability of failure occurring in the ith segment is not simply $P(\sigma_i)$. It also depends upon the probability that a more highly stressed section has not broken before the flaw in the ith section causes failure of the fibre. This is given by

The pull-out length is given by

$$l_p = \frac{l_d}{2} - x$$

and $F(x')$ is the cumulative probability of x being less than x'. Consequently the cumulative probability distribution of the pull-out length being less than or equal to l_p is

$$1-F\left(\frac{l_d}{2}-l_p\right)$$

The model assumes that the entire flaw spectrum is repeated in a length of fibre which is small by comparison with the pull-out length. This is justified since the average strength of the fibres changes only slowly with increasing gauge length. It implies that the full range of flaws must be present in short lengths of fibre.

4.2. The effect of the reinforcement on the nature of pull-out

For certain composites the debonding of single fibres does not occur because the debond stress is greater than the fibre strength. This behaviour is anticipated in materials with a strong fibre–matrix

*An allowance for the probability of a severe flaw causing fracture in a section under lower stress, before fibre failure occurs in section i, is made by the use of the *cumulative* Weibull distribution $P(\sigma)$.

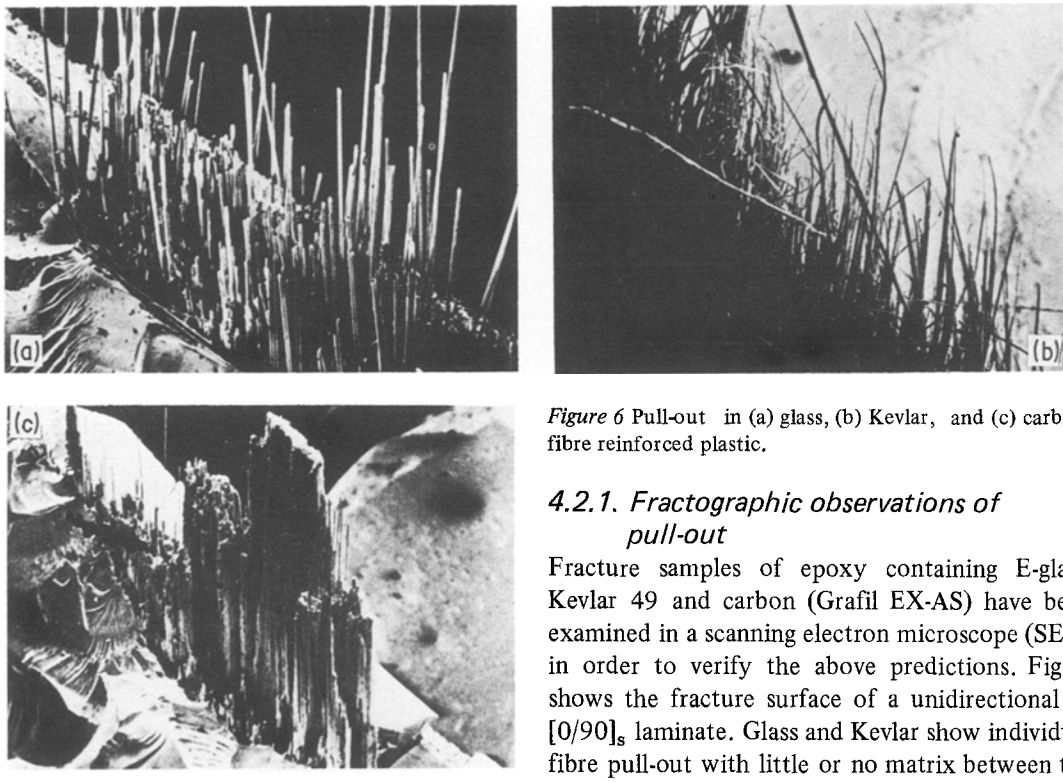

Figure 6 Pull-out in (a) glass, (b) Kevlar, and (c) carbon-fibre reinforced plastic.

bond or high fibre stiffness, as found in carbon-fibre reinforced systems. In such cases the pull-out of individual fibres is not possible, but instead a bundle of fibres (which debonds more easily than the individual fibres) behaves as a large fibre. Although a composite, the bundle still has a variable strength which can be described by a Weibull distribution with a Weibull modulus about 3.5 times larger than the single fibre, and a strength of about 80% of the rule of mixture prediction (Harlow and Pheonix [10]). The stress distribution in the bundle is similar to that in the single fibre (Section 3).

The nature of the pull-out process is therefore controlled by the debonding process. If fibres can debond, they will pull-out individually. Glass and Kevlar† should normally do this. However, if only the bundle debonds then the bundle will fracture away from the matrix crack plane and pull-out as a small piece of intact composite; this is what CFRP is predicted to do. The process may be analysed using Equation 11 when the appropriate substitutions are made. In general, a composite may show a combination of the two types of pull-out.

4.2.1. Fractographic observations of pull-out

Fracture samples of epoxy containing E-glass, Kevlar 49 and carbon (Grafil EX-AS) have been examined in a scanning electron microscope (SEM) in order to verify the above predictions. Fig. 6 shows the fracture surface of a unidirectional or $[0/90]_s$ laminate. Glass and Kevlar show individual fibre pull-out with little or no matrix between the fibres. By contrast, the carbon-fibre reinforced epoxy shows a solid bundle which has fractured and pulled out with intact matrix binding the fibres. These observations are in agreement with the debonding behaviour predicted in Section 4.2, although variations in the properties of the fibre–matrix bond could allow the other mode of pull-out to occur.

4.3. Comparison of predicted and observed distributions in composites

For a typical composite with brittle fibre reinforcement the function $P(\sigma)$ is of the Weibull form (Equation 9), and for a debonded fibre the stress distribution is

$$\sigma(x) = \sigma_p - (\sigma_p - \sigma_d)e^{-\beta x}$$

The integral (Equation 11) has been evaluated numerically for various materials and the predictions compared with experiment.

4.3.1. Results for glass-fibre reinforced plastic (GFRP)

Beaumont and Anstice [11] measured a large number of pull-out lengths in GFRP in an effort to

† Although Kevlar is a polymeric fibre it appears to behave as a brittle material. In the absence of any detailed information, the Weibull distribution (with a Weibull modulus equal to that of glass and carbon) is used to characterize the fibre strength.

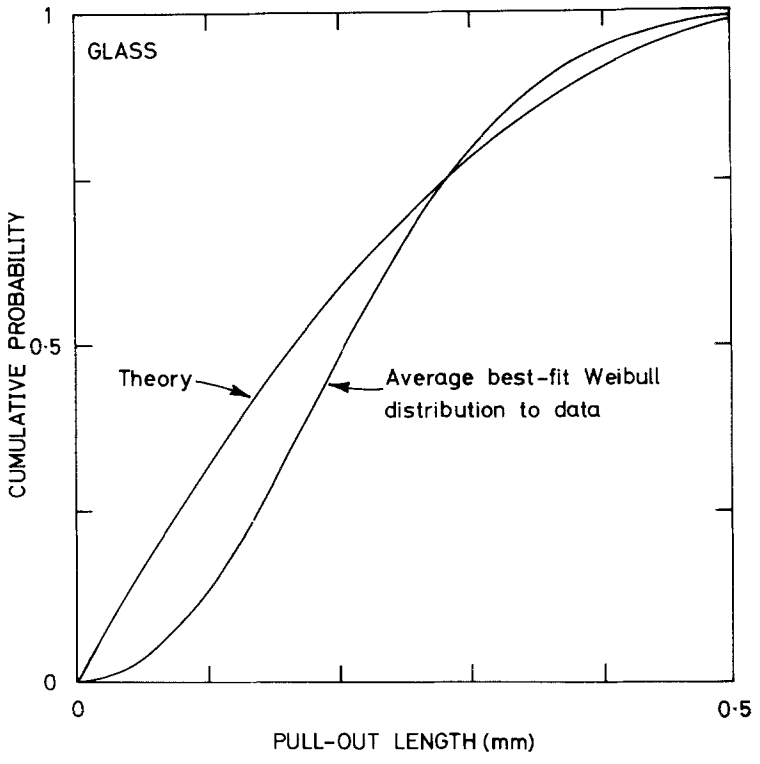

Figure 7 Predicted and best-fit Weibull distributions for fibre pull-out lengths in GFRP: $\epsilon_0 = 0.75\%$.

ascertain their distribution. The pull-out lengths were well described by a Weibull distribution, but of a much lower modulus than for the fibre strength distribution. The average of the Weibull parameters from over 2000 measurements of pull-out lengths are

$$\bar{l}_0 = 0.24 \pm 0.08\,\text{mm}$$
$$\bar{m} = 2.2 \pm 0.42$$

This distribution is shown in Fig. 7 and is compared with the prediction of Equation 11, using typical E-glass/epoxy properties listed in Table II. Good agreement is found between the predicted and experimental distributions except at small pull-out lengths. The model predicts that the most probable pull-out length (the point at which the slope is maximized) is at $l_p = 0$, which is intuitively correct since the stress is maximized at that point. By comparison, the Weibull distribution predicts zero probability of zero-length pull-outs.

4.3.2. Results for carbon-fibre reinforced plastic (CFRP)

The procedure described in Section 4.3.1 has been applied to bundle pull-out of high-strength carbon fibres using data from Wells [8]. Characteristic Weibull parameters for 500 measurements were

$$\bar{l}_0 = 0.47 \pm 0.03\,\text{mm}$$
$$\bar{m} = 1.9 \pm 0.1$$

This distribution is shown in Fig. 8, and may be compared with the result from Equation 11 using typical values for carbon fibre in epoxy (see Table II) and a bundle misfit strain of 3%. The main differences in shape of the distributions, noted in Section 4.3.1, are evident although agreement between average values is good.

4.4. A method for the rapid calculation of pull-out lengths

So far the theory has successfully predicted the shape and position of the cumulative probability distributions for both individual fibre and bundle pull-out cases. However, calculations of the complete probability distribution is time-consuming, and often an average value of the pull-out length is all that is required. Consequently the effect of changing composite properties on the shape and position of the distribution has been investigated, and correlations between pull-out and debond lengths have been sought as a means of convenient prediction.

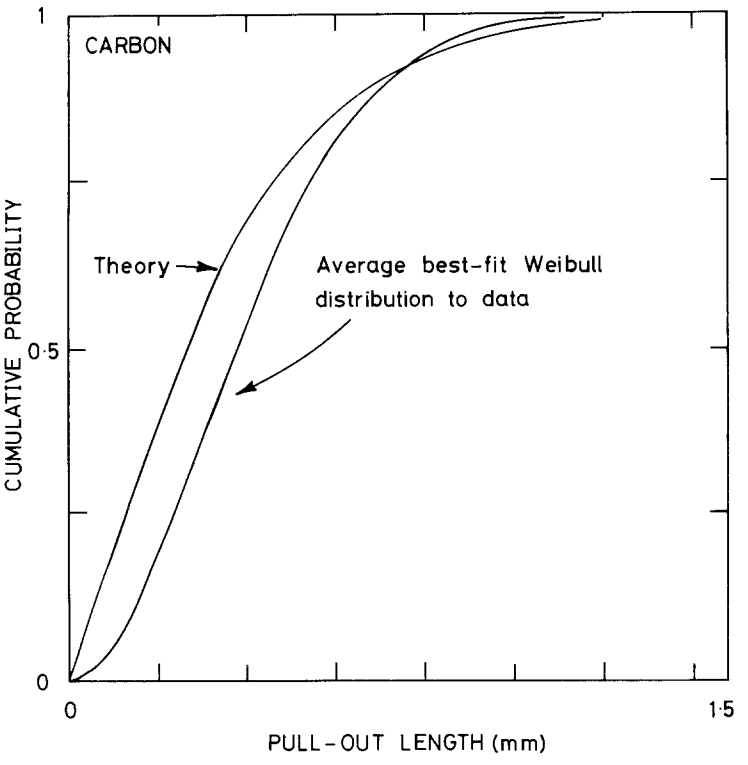

Figure 8 Predicted and best-fit Weibull distributions for bundle pull-out lengths in CFRP: $\epsilon_b = 3\%$.

4.4.1. Effect of varying material properties on pull-out distributions

From Equation 11, the pull-out length distribution is affected by any parameters which reflect changes in the flaw or stress distributions in the fibre. Changes in most of these parameters will also affect the debond length. Fig. 9 shows the effect of varying fibre misfit strain, Weibull modulus, fibre strength and radius on the probability distribution, using values which are otherwise typical of an E-glass/epoxy composite. In particular, it should be noted that the distribution is relatively insensitive to the Weibull modulus.

4.4.2. Correlation between fibre pull-out and fibre debond length

Fig. 10 shows the relationship between the average pull-out length $\bar{l}_p$ and the fibre debond length l_d (as calculated using Equation 6) when several parameters vary. The average pull-out length for both glass and Kevlar reinforced material may be estimated by

$$\bar{l}_p = \frac{l_d}{6.8}$$

This approximation is accurate to within ± 10% for $l_p < 0.3$ mm (or $l_d < 2.1$ mm). The behaviour due to changing G_1, and therefore the debond stress, is least well predicted.

4.4.3. Correlation between bundle pull-out and bundle debond length

Fig. 11 shows a similar variation between pull-out and debond lengths for typical high-strength carbon-fibre composite. There is a correlation between l_p and l_d for changes of fibre strength, radius and fibre misfit strain. However, as noted in the previous section, changes due to variations in debond stress do not follow the same trend. Nevertheless an approximate relationship may be found in the region $0.22\,\text{mm} < \bar{l}_p < 0.32\,\text{mm}$, or $7.5\,\text{mm} < l_d < 12\,\text{mm}$, to an accuracy of ± 20%, namely

$$\bar{l}_p = \frac{l_d}{35} \qquad (12)$$

5. Summary and conclusions

1. The energy absorption in composites is dependent on the length of debonding and pull-out. These processes have been studied to enable the lengths to be calculated from fibre, resin and interface properties.

2. The study shows that two types of debonding are possible, namely single-fibre and

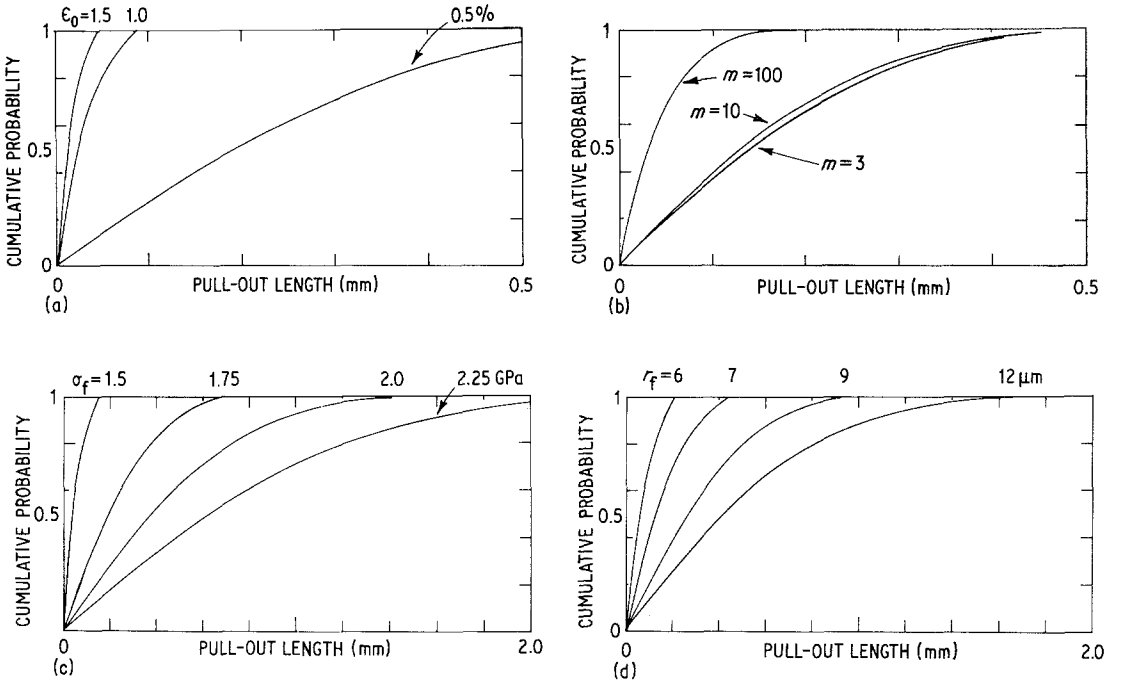

Figure 9 Effect of changing material parameters on fibre pull-out distribution in GFRP. Parameter varying: (a) misfit strain, (b) Weibull modulus, (c) fibre strength, and (d) fibre radius.

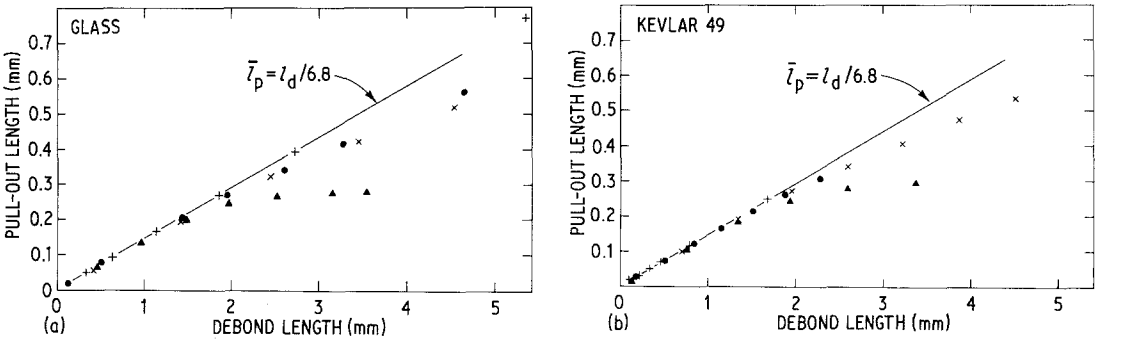

Figure 10 Correlations between fibre pull-out and debond lengths for (a) glass, (b) Kevlar-reinforced material.

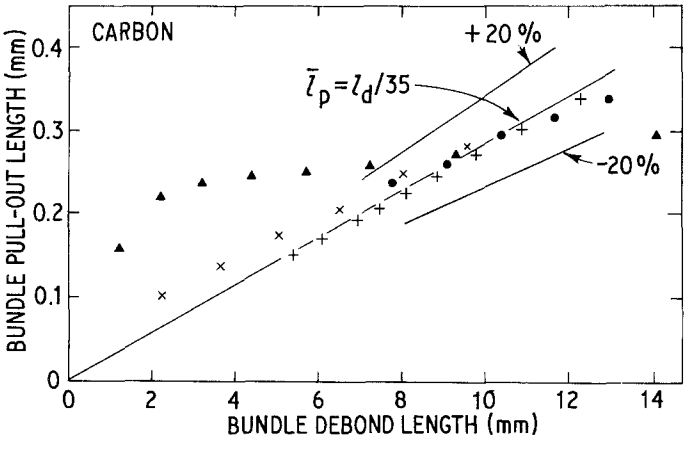

Figure 11 Predicted correlation between bundle pull-out and debond lengths for high-strength carbon-fibre composite (see Fig. 10 for key).

bundle debonding. Debond lengths have been measured and found to be in agreement with the predictions of the theory.

3. A model has been proposed for the fracture of brittle fibres under non-uniform stress, predicting the probability of fracture sites. As a result of the two types of debonding (single-fibre and bundle), two corresponding modes of pull-out have been proposed and observed in practice.

Acknowledgements

The authors wish to acknowledge helpful discussions with Professor M. F. Ashby. One of us (JKW) acknowledges the support of the Science and Engineering Research Council in the form of a Research Studentship during the course of this work.

References

1. A. KELLY, *Proc. Roy. Soc.* **A282** (1964) 63.
2. D. H. KAELBLE, *J. Adhesion* **5** (1973) 245.
3. J. N. KIRK, M. MUNRO and P. W. R. BEAUMONT, *J. Mater. Sci.* **13** (1978) 2197.
4. L. B. GRESZCZUK, ASTM STP 452 (American Society for Testing and Materials, Philadelphia, 1969) p. 42.
5. P. J. LAWRENCE, *J. Mater. Sci.* 7 (1972) 1.
6. A. TAKAKU and R. G. C. ARRIDGE, *J. Phys. D: Appl. Phys.* **6** (1973) 2038.
7. J. D. OUTWATER and M. C. MURPHY, Paper 11c, 24th Annual Technical Conference on Composites (The Society of the Plastics Industry, New York, NY, 1969).
8. J. K. WELLS, PhD thesis, Cambridge University (1982).
9. B. HARRIS, *J. Mater. Sci.* **13** (1978) 173.
10. D. G. HARLOW and S. L. PHEONIX, *J. Comp. Mater.* **12** (1978) 195.
11. P. W. R. BEAUMONT and P. D. ANSTICE, *J. Mater. Sci.* **15** (1980) 2619.

Received 28 June
and accepted 10 July 1984